The Journal of Experimental Biology 209, 3529-3544
Published by The Company of Biologists 2006
doi:10.1242/jeb.02419

Molecular characterization of sodium/proton exchanger 3 (NHE3) from the yellow fever vector, *Aedes aegypti*

Ashok K. Pullikuth[1,*,†], Karlygash Aimanova[1,*], Wanyoike Kang'ethe[2], Heather R. Sanders[1,3,‡] and Sarjeet S. Gill[1,2]

[1]*Department of Cell Biology and Neuroscience, Graduate Programs in* [2]*Environmental Toxicology and* [3]*Microbiology, University of California, Riverside, CA 92521-0146, USA*

*These authors contributed equally to this work

†Author for correspondence at present address: Department of Pharmacology and Experimental Therapeutics, Louisiana State University, School of Medicine, 1901 Perdido Street, New Orleans, LA 70112, USA (e-mail: apulli@lsuhsc.edu)

‡Present address: Invitrogen Corporation, Carlsbad, CA 92008, USA

Accepted 29 June 2006

Summary

Transport across insect epithelia is thought to depend on the activity of a vacuolar-type proton ATPase (V-ATPase) that energizes ion transport through a secondary proton/cation exchanger. Although several of the subunits of the V-ATPase have been cloned, the molecular identity of the exchanger has not been elucidated. Here, we present the identification of sodium/proton exchanger isoform 3 (NHE3) from yellow fever mosquito, *Aedes aegypti* (*Ae*NHE3). *Ae*NHE3 localizes to the basal plasma membrane of Malpighian tubule, midgut and the ion-transporting sector of gastric caeca. Midgut expression of NHE3 shows a different pattern of enrichment between larval and adult stages, implicating it in the maintenance of regional pH in the midgut during the life cycle. In all tissues examined, NHE3 predominantly localizes to the basal membrane. In addition the limited expression in intracellular vesicles in the median Malpighian tubules may reflect a potential functional versatility of NHE3 in a tissue-specific manner. The localization of V-ATPase and NHE3, and exclusion of Na^+/K^+-ATPase from the distal ion-transporting sector of caeca, indicate that the role of NHE3 in ion and pH regulation is intricately associated with functions of V-ATPase. The *Ae*NHE3 complements yeast mutants deficient in yeast NHEs, NHA1 and NHX1. To further examine the functional property of *Ae*NHE3, we expressed it in NHE-deficient fibroblast cells. *Ae*NHE3 expressing cells were capable of recovering intracellular pH following an acid load. The recovery was independent of the large cytoplasmic region of *Ae*NHE3, implying this domain to be dispensable for NHE3 ion transport function. $^{22}Na^+$ uptake studies indicated that *Ae*NHE3 is relatively insensitive to amiloride and EIPA and is capable of Na^+ transport in the absence of the cytoplasmic tail. Thus, the core domain containing the transmembrane regions of NHE3 is sufficient for pH recovery and ion transport. The present data facilitate refinement of the prevailing models of insect epithelial transport by incorporating basal amiloride-insensitive NHE3 as a critical mediator of transepithelial ion and fluid transport and likely in the maintenance of intracellular pH.

Key words: NHE antiporter, midgut, Malpighian tubule, insect epithelia.

Introduction

Blood-feeding insects such as adult mosquitoes face an enormous challenge to void excess fluid imbibed from their vertebrate host. An exquisite interplay of hormonal and membrane transport processes facilitates rapid removal of excess ions and fluid from the insect hemolymph. Although the physiology of such diuretic mechanisms has been appreciated since the early studies (Ramsay, 1950; Wigglesworth, 1972), the molecular detail surrounding this efficient diuretic system remains largely elusive. In vertebrate models systems, a sodium/potassium ATPase (Na^+/K^+-ATPase) appears to play a critical role in facilitating membrane transport. This sodium motive paradigm is widely accepted. However, studies by Harvey and Wieczorek and their colleagues in insect epithelia indicate that a proton-motive transport process might be a key determinant in transport (Wieczorek et al., 2000). In lepidoteran midgut, the protons extruded from the cell into the lumen by vacuolar-type ATPase (V-ATPase) dictate ion transport through a functionally coupled potassium pump (K-pump or antiporter). The activities of V-ATPase together with the K-pump are crucial to maintain an alkaline midgut in lepidoptera (Dow, 1999; Wieczorek et al., 1999).

Pharmacological studies in various insect epithelia indicate the K-transport component to be reminiscent of sodium/proton exchangers (NHEs) that regulate intracellular pH as well as a variety of other functions in vertebrates (Burckhardt et al., 2002; Counillon and Pouyssegur, 2000; Grinstein and Wieczorek, 1994; Orlowski and Grinstein, 2004). However, no NHE 'isoform' has been molecularly characterized in any insect system, although some studies have suggested their existence in some insect tissues involved in ion transport (Giannakou and Dow, 2001; Hart et al., 2002; Pannabecker, 1995; Petzel, 2000)

Given the importance of NHEs in regulating cellular and systemic pH, and ion transport and their potential to be functionally coupled to the activities of V-ATPases, molecular identification of members of this family is required in order to formulate a comprehensive model to understand how mosquitoes efficiently regulate ion and fluid balance following a blood meal. The cascades culminating in and initiated through these processes are crucial for the reproductive biology of mosquitoes and for disease transmission vectored by these insects.

Ion transport studies in insect epithelia show that the primary active transport of H^+ by a V-ATPase drives secondary ion transport through Na^+ or K^+/H^+ exchanger(s) that together function as primary generators of electrochemical gradients (Pannabecker, 1995; Wieczorek, 1992). Protons extruded by V-ATPase into the lumen are cycled by the exchangers allowing K^+ (or Na^+) and fluid secretion (Pannabecker, 1995; Wieczorek, 1992). Implicit in this model is that the K^+ (or Na^+)/H^+ exchanger virtually operates in reverse to pump H^+ from the lumen in to the cell, which is a property exploited in vertebrate epithelial cells to clone NHE-deficient cell lines (Paris and Pouyssegur, 1983; Pouyssegur et al., 1984). The molecular identity of these Na^+ or K^+/H^+ exchangers has been suggested from pharmacological studies on isolated Malpighian tubules (Petzel, 2000), or from the recently completed insect genome sequences (Adams et al., 2000; Holt et al., 2002; Pullikuth et al., 2003).

The Malpighian tubules of insects are robust ion- and fluid-transporting tissues (Maddrell and O'Donnell, 1992; Maddrell, 1991), and in the mosquito *Aedes aegypti*, Malpighian tubules secrete 0.4 nl min^{-1} spontaneously. When stimulated with natriuretic peptides (MNP) or cAMP, tubules secrete at a rate of 2.8 nl min^{-1}, simulating secretion rates after a blood meal (Petzel et al., 1987; Petzel et al., 1986). Microfluorimetric and microelectrode measurements showed the rapid secretion, which is coupled to a bafilomycin-sensitive V-ATPase, is sensitive to amiloride or its analogs; these features are reminiscent of a Na^+ or K^+/H^+ exchanger (Beyenbach et al., 2000; Petzel, 2000). Further, NHE antagonists reduced recovery of pH_i following an acid load in isolated Malpighian tubules (Petzel et al., 1999). Thus, pH_i regulation by exchangers is directly linked to the fluid secreting efficiency of tubules.

The mosquito, *Ae. aegypti*, is a vector of human diseases including hemorrhagic dengue fever and yellow fever. Ingestion of a blood meal by the adult female results in an enormous Na^+ load and increase in fluid volume, both of which have to be regulated rapidly. Although prevailing models suggest the involvement of NHE-like proteins in regulating ionic and fluid secretion in mosquitoes, their diversity, cellular expression, localization, functions and/or sensitivity to inhibitors remain incompletely understood in these insects. Here we present the molecular and functional characterization of *Ae. aegypti* NHE3 (GenBank accession numbers reported are AF187723). We show that *Ae*NHE3 complements yeast NHE and heterologous expression in NHE-deficient epithelial cells results in the transport of $^{22}Na^+$ and in the recovery of pH_i after an acid load. Immunohistochemical evidence for its localization in the basolateral plasma membrane domain suggests that current models of ion transport in Malpighian tubules need to be re-evaluated.

Materials and methods

Cell lines and reagents

Restriction and DNA modifying enzymes were from New England Biolabs. Cyanine3 (Cy3)- and Cy5-conjugated secondary antibodies were from Jackson ImmunoResearch Laboratories. A sodium/proton exchanger activity deficient cell line (PS120) derived from Chinese hamster lung fibroblast cell line CCL39 was obtained from Dr James Melvin (Attaphitaya et al., 1999) (University of Rochester, Rochester, NY, USA) with the kind permission of Dr Jacques Pouyssegur (Centre Antoine Lacassagne, Nice, France) (Pouyssegur et al., 1984). A dual-function expression vector, pXOON, was a gift from Dr Thomas Jespersen (University of Copenhagen, Denmark) (Jespersen et al., 2002). Nigericin, Alexa Fluor 488-phalloidin and 2′,7′-bis-(2-carboxyethyl-5-(and-6)-carboxyfluorescein, acetoxymetyl ester (BCECF-AM) were purchased from Molecular Probes. Geneticin (G418) and cell culture reagents were from Invitrogen (Carlsbad, CA, USA). Carrier free $^{22}Na^+$ was purchased from Amersham Biosciences (Piscataway, NJ, USA). Unless stated otherwise, all other reagents were purchased from Sigma-Aldrich.

Isolation of NHE3 cDNA and analysis of protein sequence

Partial cDNAs were obtained using degenerate primers to conserved NHE amino acid sequences, LDAGYFMP and AVDPVAVFE, and mRNA isolated from the midgut and Malpighian tubules of *Aedes aegypti* L. Gene specific primers were then designed and used for screening an *Ae. aegypti* Malpighian tubule cDNA library as described (Ross and Gill, 1996). The cDNA clone isolated was sequenced completely in both directions to obtain the nucleotide and deduced amino acid sequences.

Transmembrane predictions were inferred from SOSUI analysis at Sosui/proteome.bio.tuat.ac.jp (Hirokawa et al., 1998). Potential phosphorylation sites were identified through high stringency scans by NetPhos and ScanSite algorithms at www.cbs.dtu.dk and scansite.mit.edu respectively. Gene structure analysis was performed with *Aedes aegypti* NHE3 ORF against the recently released *Ae. aegypti* WGS scaffolds.

Expression of Aedes aegypti NHE3 in Saccharomyces cerevisiae

S. cerevisiae strains G19 (MATα, ade2, his3, leu2, trp1, ura3, Δena1::HIS3::ena4) and AXT3 (MATα, ade2, his3, leu2, trp1, ura3, Δena1::HIS3::ena4, nha1::LEU2, nhx1::TRP1) were gifts from Dr Jose M. Pardo (Consejo Superior de Investigaciones Cientificas, Sevilla, Spain) and have been previously characterized (Madrid et al., 1998; Quintero et al., 2000). Both strains are derivatives of W303-1B (MATα, ura3-1 leu2-3, 112his3-11, 15trp1-1, ade2-1, can1-100). pYES2.1 TOPO: Aedes NHE3 plasmid was transformed into yeast cells following the LiCl method. Growth in high Na^+ was assayed in alkali cation-free arginine phosphate (AP) medium (Rodriguez-Navarro and Ramos, 1984) containing known concentrations of NaCl. Tolerance to hygromycin B was assayed in minimal medium.

Constructs for cell line expression

The *Aedes* NHE3 ORF was amplified using Expand Hi-Fidelity PCR system (Roche Biochemicals, Indianapolis, IN, USA) and cloned as two separate fragments into pXOON vector (Jespersen et al., 2002). First, a 2.2 kb 5′ fragment of ORF that codes for the N-terminal 731 amino acids was cloned in to a dual expression vector pXOON (designated NHE-731Δ). NHE-731Δ lacks the C-terminal cytoplasmic tail but contained the sequence (^{732}TGDIGPAGHDRAAA stop) that was coded by the cloning site and the vector followed by several in-frame stop codons. Second, a 1.2 kb fragment coding for the C-terminal tail was seamlessly appended to NHE-731Δ to reconstitute the full-length *Aedes* NHE3 ORF. The expression vector pXOON also codes for EGFP from a different promoter site enabling isolation of transfected cells by GFP fluorescence. All constructs were fully sequenced to confirm that no PCR errors were introduced.

Stable cell lines expressing Aedes aegypti NHE3

PS120 cells (Pouyssegur et al., 1984) in Dulbecco's modified Eagle medium (DMEM) supplemented with penicillin/streptomycin/fungizone (Invitrogen) and 10% fetal bovine serum (FBS) were transfected using Lipofectamine 2000 (Invitrogen) either with 5–12 μg of *Pme*I linearized expression constructs or vector alone. After 2 days, selection medium containing G418 (1 mg ml^{-1}) (in DMEM, 10% fetal bovine serum and antibiotics) was added and growth maintained until individual foci were apparent. Transfected cells were also selected with HBS (20 mmol l^{-1} Hepes-KOH, 5 mmol l^{-1} glucose, 2 mmol l^{-1} $CaCl_2$, 5 mmol l^{-1} KCl, 1 mmol l^{-1} $MgCl_2$) buffered HCO_3^--free DMEM, pH 6.9 to hasten the selection process. The parental PS120 cells are conditional for growth in bicarbonate-free medium (Pouyssegur et al., 1984) at acidic and neutral pH. Therefore, clones that survived the acid challenge in selection medium contained functionally expressed NHE. Fifteen independent clonal lines were selected for each NHE expression construct. Clones were initially assayed for recovery of intracellular pH (pH_i) with the cell-permeant fluorescent pH indicator, 2′,7′-bis-(2-carboxyethyl-5-(and-6)-carboxyfluorescein, acetoxymetyl ester (BCECF-AM: Molecular Probes) as described for measurement of pH_i below. Selected clones were expanded and frozen or maintained in selection medium. Alternatively, 2 weeks after transfection, plates were incubated in HCO_3^--free DMEM for 3–8 days, dead cells were removed and viable cells trypsinized and maintained as polyclonal populations in medium containing G418 (1 mg ml^{-1}).

Assay for $^{22}Na^+$ uptake

PS120 cells were cultured in bicarbonate buffered DMEM with 10% fetal calf serum. At 90–95% confluency each 10 cm^2 plate was trypsinized. The cell pellet was resusupended in culture medium and equal volumes added to each well in a 24-well plate. The day after plating, cells were transfected with 0.8 μg plasmid DNA with Lipofectamine 2000 (Invitrogen) according to manufacturer's recommendation. Uptake assays were performed 2–3 days after transfection. Culture medium was aspirated and wells washed quickly twice with 1 ml of acid load buffer (50 mmol l^{-1} NH_4Cl, 70 mmol l^{-1} choline chloride, 1 mmol l^{-1} $MgCl_2$, 2 mmol l^{-1} $CaCl_2$, 5 mmol l^{-1} glucose, 20 mmol l^{-1} Hepes-Tris, pH 7.4) and incubated in 0.5 ml of the same buffer for 30 min at 37°C (in nominal CO_2) (Orlowski, 1993; Wakabayashi et al., 1992). Cells were washed twice and incubated for 5 min at room temperature in choline chloride buffer (135 mmol l^{-1} choline chloride, 1 mmol l^{-1} $MgCl_2$, 2 mmol l^{-1} $CaCl_2$, 5 mmol l^{-1} glucose, 20 mmol l^{-1} Hepes-Tris, pH 7.4). To initiate $^{22}Na^+$ uptake, buffer solution was aspirated and 250 μl of uptake buffer was added and incubated for 20 min at room temperature. Uptake buffer contained 1 μCi ml^{-1} (1 Ci=3.7×10^{10} Bq) of carrier-free $^{22}Na^+$ in choline chloride buffer supplemented with 1 mmol l^{-1} ouabain and 100 μmol l^{-1} bumetanide from 0.5 mol l^{-1} and 0.1 mol l^{-1} stocks in 100% DMSO, respectively. Uptake was stopped by adding 1 ml of ice-cold stop solution (135 mmol l^{-1} NaCl, 1 mmol l^{-1} $MgCl_2$, 2 mmol l^{-1} $CaCl_2$, 5 mmol l^{-1} glucose, 4 mmol l^{-1} KCl, 20 mmol l^{-1} Hepes-Tris, pH 7.4) and quickly rinsed four times with the same solution. Cells were solubilized in 0.5 ml of 0.5 mol l^{-1} NaOH and added to 0.5 ml of 0.5 mol l^{-1} HCl wash collected after rinsing the wells (Orlowski, 1993). Both were pooled, added to 2–4 ml of scintillation fluid and counted. A 50 μl sample of NaOH- and Hcl-extracted and pooled samples was saved for protein estimation with BCA reagent (Pierce, Rockford, IL, USA) with bovine serum albumin (BSA) as standard. The effect of inhibitors was assessed by adding appropriate amounts from stock solutions made in 100% DMSO. An equivalent volume of solvent was added to control wells to account for any carrier effect on uptake. Data were normalized to protein concentration in each well.

Antibodies

Monoclonal antibody to avian Na^+/K^+-ATPase (Takeyasu et al., 1988) was obtained from the Developmental Studies Hybridoma Bank, University of Iowa, IA, USA). Polyclonal antibody to B-subunit of vacuolar ATPase (V-ATPase) has

been previously described (Filippova et al., 1998). A purified synthetic peptide corresponding to the C-terminal residues (E^{1111}→G^{1128}) of *Aedes* NHE3 with an N-terminal cysteine was synthesized at Molecular Genetic Instrumentation Facility (University of Georgia, GA, USA). The synthetic peptide was conjugated to maleimide-activated KLH (Pierce) and used to immunize rabbits for antibody production. Production bleeds with highest titers, determined by ELISA, were used for immunohistochemical studies.

Tissue preparation for immunohistochemistry

Fourth instar larvae and adult female *Aedes aegypti* were dissected in PBS and fixed overnight in 4% paraformaldehyde (PFA) at 4°C. Tissues were washed in PBS and dehydrated for 3–6 h each in 20, 40, 70 and 96% ethanol followed by three changes in 100% ethanol at room temperature. Ethanol was replaced with a xylene series (30% and 70%) and with two changes in 100% for 6–16 h at each step. Paraplast chips were added to tissues in xylene and incubated at 58°C, followed by complete infiltration with 100% paraplast. Microtome sections of 8 μm were cut and adhered to silane-prep slides (Sigma-Aldrich).

Immunohistochemistry

Tissue sections were deparaffinated with xylene, rehydrated in a descending ethanol series and washed with PBS-Triton X-100 (PBS-Tx; 0.1%Triton X-100, 1×PBS, pH 7.4). Sections were blocked with 2%BSA for 2 h at room temperature. The appropriate dilution of antibodies (in PBS-Tx) were added after blocking and incubated at 4°C overnight. Unbound material was removed and tissues further blocked in 2% normal goat serum (NGS). Cy3- or Cy5-conjugated to either anti-rabbit or anti-mouse antibodies diluted in PBS-Tx were used as secondary antibodies. After 1–2 h of incubation with secondary antibody in the dark, tissues were washed with PBS-Tx and mounted for microscopic examination in 90%glycerol/4%*N*-propyl gallate.

Double labeling of NHE3 and Na^+/K^+-ATPase

Dual labeling experiments were done using whole rabbit serum against *Aedes* NHE3 (1:250 dilution) and mouse anti-avian Na^+/K^+-ATPase antibody (a5 culture supernatant, 1:10 dilution). In all experiments, preimmune serum, or antibody preabsorbed with antigen, were used as negative controls. Whole-mount immunohistochemistry was performed with similarly fixed and blocked tissues. Anti-NHE3 and anti-Na^+/K^+-ATPase antibodies were used at 1:500 and 1:20 dilution, respectively.

Confocal microscopy and image acquisition

Sections and whole mounts were examined with a Zeiss Axioplan confocal microscopy (LSM510) at the Center for Advanced Microscopy and Microanalysis at University of California, Riverside, CA, USA. All images were imported to Adobe Photoshop (6.0) where final assembly and labeling were done.

Buffers and inhibitors

Insect saline contained 156 mmol l^{-1} NaCl, 6 mmol l^{-1} KCl, 5 mmol l^{-1} glucose, 2 mmol l^{-1} $CaCl_2$, 1 mmol l^{-1} $MgCl_2$ and 20 mmol l^{-1} Hepes-KOH, pH 7.3 (Petzel et al., 1999). Other solutions were prepared in Hepes-buffered saline (HBS: 20 mmol l^{-1} Hepes-KOH, pH 7.4, 5 mmol l^{-1} KCl, 1 mmol l^{-1} $MgCl_2$, 2 mmol l^{-1} $CaCl_2$, 5 mmol l^{-1} glucose). Normal sodium medium was prepared in HBS containing 135 mmol l^{-1} NaCl. For sodium-free medium, NaCl was replaced with 135 mmol l^{-1} *N*-methyl-D-glucamine (NMDG). Ouabain was prepared as 10 mmol l^{-1} stock in HBS or choline chloride buffer. Bumetanide was prepared as 0.1 mol l^{-1} stock in 100% dimethyl sulfoxide (DMSO).

Measurement of intracellular pH (pH_i)

Cells were plated at a density of 30–50×10^4 per well in 48-well culture plates and grown in DMEM with 10% FBS, penicillin/streptomycin/fungizone (Invitrogen) with or without G418 (1 mg ml^{-1}) for transfected and untransfected cells, respectively. Two days after plating, the culture medium was aspirated, wells washed with normal sodium buffer twice and loaded with the fluorescent indicator dye BCECF (5 μmol l^{-1} in 135 mmol l^{-1} NaCl, HBS, pH 7.4) for 30 min at 37°C. Cells were pulsed with ammonium chloride (60 mmol l^{-1} NH_4Cl, 75 mmol l^{-1} NaCl, in HBS, pH 7.4) for 10 min at 37°C. To increase intracellular acidity, cells were then washed with sodium-free medium (HBS, pH 7.3, 135 mmol l^{-1} NMDG) twice and incubated further for 5 min at room temperature. Appropriate buffers were then added and intracellular change in BCECF fluorescence monitored as end-point measurements after 7–10 min. Plates were scanned in a Typhoon 9410 variable mode imager (Molecular Dynamics, Sunnyvale, CA, USA) equipped with blue laser with dual excitation of 457 and 488 nmol l^{-1} and emission recorded through a 555 band pass 20 nmol l^{-1} filter. Plates were scanned at a resolution of 200 μm and images acquired by ImageQuant 5.1 software, exported as Microsoft Excel spread sheet and analyzed in Microcal Origin 6.1. Calibration of pH_i was performed by high KCl/nigericin technique (Zhang et al., 1992). Briefly, cells were incubated with 10 μmol l^{-1} nigiricin containing KCl buffers (HBS, 150 mmol l^{-1} KCl) adjusted for pH between 5.5 and 8.0. Duplicate wells in each plate were used for each pH value (total of 8 points in the range). Emissions at pH-insensitive excitation of 457 and pH-sensitive excitation of 488 were derived as ratios and converted to pH values by a mathematical fit. A calibration curve from each plate was used to determine the pH_i in experimental wells. The contributions of Na^+/K^+-ATPase and $Na^+/K^+/Cl^-$ cotransporters to ion influx was determined by incubating cells in parallel with buffers containing 1 mmol l^{-1} ouabain and 100 μmol l^{-1} bumetanide, respectively.

Results

Cloning and sequence analysis of Aedes aegypti NHE3

Degenerate primers toward conserved vertebrate NHE sequences were used to isolate a PCR product from the midgut

and Malpighian tubules mRNA of *Aedes aegypti*. This partial sequence was then used to isolate a full-length cDNA coding for the *Aedes* NHE homologue from a Malpighian tubule cDNA library. The cDNA was 3981 bp long with 3540 bp (from 165 to 3704 bp) open reading frame translating to 1179 amino acids. A perfect polyadenylation signal (AAUAAA) at 3951 bp is located immediately upstream of the poly(A) tail. Our preliminary analysis of *Aedes aegypti* genome at the NHE3 locus indicates that the open reading frame is coded by 21 exons covering a rather large genome segment (ca. 154 kb) (Fig. 1A, asterisks; data not shown). Exon 1 (5′UTR + amino acids 1–182) is the largest coding exon whereas exon 2 (amino acids 183–194) is the shortest. The size of introns varies from 63 bases (between exons 9 and 10) and 31.7 kb (between exons 3 and 4).

The *Aedes* NHE protein product is estimated to be 130.2 kDa (pI=6.78) (Fig. 1A). By sequence similarity to vertebrate NHEs and evolutionary relationship to cloned NHEs (not shown) (Pullikuth et al., 2003), we assign *Aedes* NHE to the NHE3 family (hereafter, *Ae*NHE3). *Ae*NHE3 is predicted to contain 12 transmembrane helices with both N and C termini oriented cytoplasmically (Hirokawa et al., 1998). The C terminus accounts for 56% of the protein and contains several putative regulatory sites (Fig. 1B). *Ae*NHE3 apparently lacks potential *N*-glycosylation sites but contains potential sites for cAMP- and cGMP-dependent protein phosphorylation (T668, S820, S935, S1017, S1099), and casein kinase II phosphorylation (S1162). *Ae*NHE3 is likely to be phosphorylated by ERK1&2 since a consensus site (PX(S/T)P) for ERK is found at T307 within the ERK substrate motif 305PLTP308. Further, two ERK D-domains necessary for ERK docking to its substrates are embedded around V808 and L1103. The preponderance of these sites in the C-terminal tail indicates that *Ae*NHE3 function is likely regulated by phosphorylation by several kinases in metabolic, physiological and cell cycle contexts, as with many vertebrate NHEs (Counillon and Pouyssegur, 2000; Orlowski and Grinstein, 1997). *Ae*NHE3 also contains a calcineurin B homologous protein (CHP) binding site in the cytoplasmic tail (Fig. 1D) (Pang et al., 2001).

The *Ae*NHE3 protein is nearly identical to two PCR-derived *Aedes* NHEs (Hart et al., 2002) and is similar to *Drosophila* NHE2 (53%) (Giannakou and Dow, 2001) and vertebrate NHE3s (50%) (Biemesderfer et al., 1993; Brant et al., 1995; Tse et al., 1993) (Fig. 1A). Since *Drosophila* NHEs were presumably named by the order of discovery, we assign *Drosophila* NHE2, originally annotated by Giannakou and Dow to the NHE3 family (Giannakou and Dow, 2001), hence termed DmNHE3. Partially using the *Ae*NHE3 sequence reported here, Hart et al. identified two PCR products that exhibited >95% identity (Hart et al., 2002). It is interesting to note that the shorter 2.8 kb PCR product (mNHE2.8 kb), which differs at 11 positions to the longer 3.7 kb fragment (mNHE3.7 kb), ends precisely after exon 10. This data, together with the presence of a distinct 3′ UTR in the mNHE2.8 kb PCR product (Hart et al., 2002), suggests that *Ae*NHE3 is likely expressed as at least two splice variants.

Tissue distribution of AedesNHE3

Polyclonal antibodies to a C-terminal peptide (E^{1111}→G^{1128}) of *Ae*NHE3 with an added N-terminal cysteine were generated and used to examine the distribution of *Ae*NHE3 in larval and adult tissues of *Ae. aegypti*. In larvae, higher level of *Ae*NHE3 expression was detected in the distal end of posterior midgut, Malpighian tubules and hindgut (Fig. 2A), while the anterior midgut showed reduced staining for NHE3. Preimmune antibody or immune antibody preabsorbed with the C-terminal synthetic peptide antigen did not show any specific labeling (Fig. 2B). In adult mosquitoes, both anterior midgut and the proximal section of posterior midgut expressed higher levels of NHE3, together with Malpighian tubule and hindgut. Remarkably, the distal section of posterior midgut exhibited only weaker labeling (Fig. 2C). In both anterior (Fig. 2D) and posterior (Fig. 2E) midgut, NHE3 was found to localize exclusively to the basolateral domain of the plasma membrane.

In gastric caeca, NHE3 expression predominates in the distal part of caeca known to actively transport ions (Fig. 3A,B) (Ramsay, 1950; Ramsay, 1951; Volkmann and Peters, 1989a; Volkmann and Peters, 1989b). Proximal segments of caeca contained weak, if any, staining for NHE3 (Fig. 3C). Immunohistochemistry with tissue sections revealed NHE3 to localize to the basal membrane; no apical staining was detected (Fig. 3B,C). Preimmune antibody (Fig. 3D) or immune antibody preabsorbed with the peptide antigen did not show any specific labeling. Double labeling with monoclonal antibody to Na^+/K^+-ATPase indicated that NHE3 expression is characteristically segregated from Na^+/K^+-ATPase expression (Fig. 3E–G). Na^+/K^+-ATPase is abundantly expressed in the proximal segment of the caeca (Fig. 3E) and localized to the basolateral membrane (Fig. 3F). In proximal and distal caecal cells, the V-ATPase localizes predominantly to the apical side (Fig. 3H,I), whereas in distal cells weaker staining was also detected in the basal side (Fig. 3H).

Ion and fluid transport in the Malpighian tubule is energized by a proton pump that combines a V-ATPase and a secondary ion transport system that returns luminal protons in exchange for cellular Na^+ or K^+ (Beyenbach, 1995; Pannabecker, 1995). Staining of Malpighian tubules with antibodies to B-subunit of the V-ATPase revealed that V-ATPase is primarily located in the apical membrane, consistent with its proposed role in proton secretion (Fig. 4A,B). Similar to gastric caeca and midgut, NHE3 localized to the basolateral membrane of Malpighian tubules in the proximal segment (Fig. 4D). Cytoplasmic staining as punctate structures were also evident in the Malpighian tubule, possibly representing an intracellular pool of NHE3 (Fig. 4F). Basolateral expression of NHE3 reflects the localization pattern of Na^+/K^+-ATPase. In the principal ion-secreting cells in proximal tubules, Na^+/K^+-ATPase colocalized with NHE3 to the basal membrane (Fig. 4F). Interestingly, we also detected apical staining for NHE3 in median Malpighian tubule that appeared unique for this segment, as proximal and distal ends of the tubules showed only basal membrane staining with NHE3 antibody (Fig. 4E). Although hindgut expressed NHE3, the intensity of staining

A

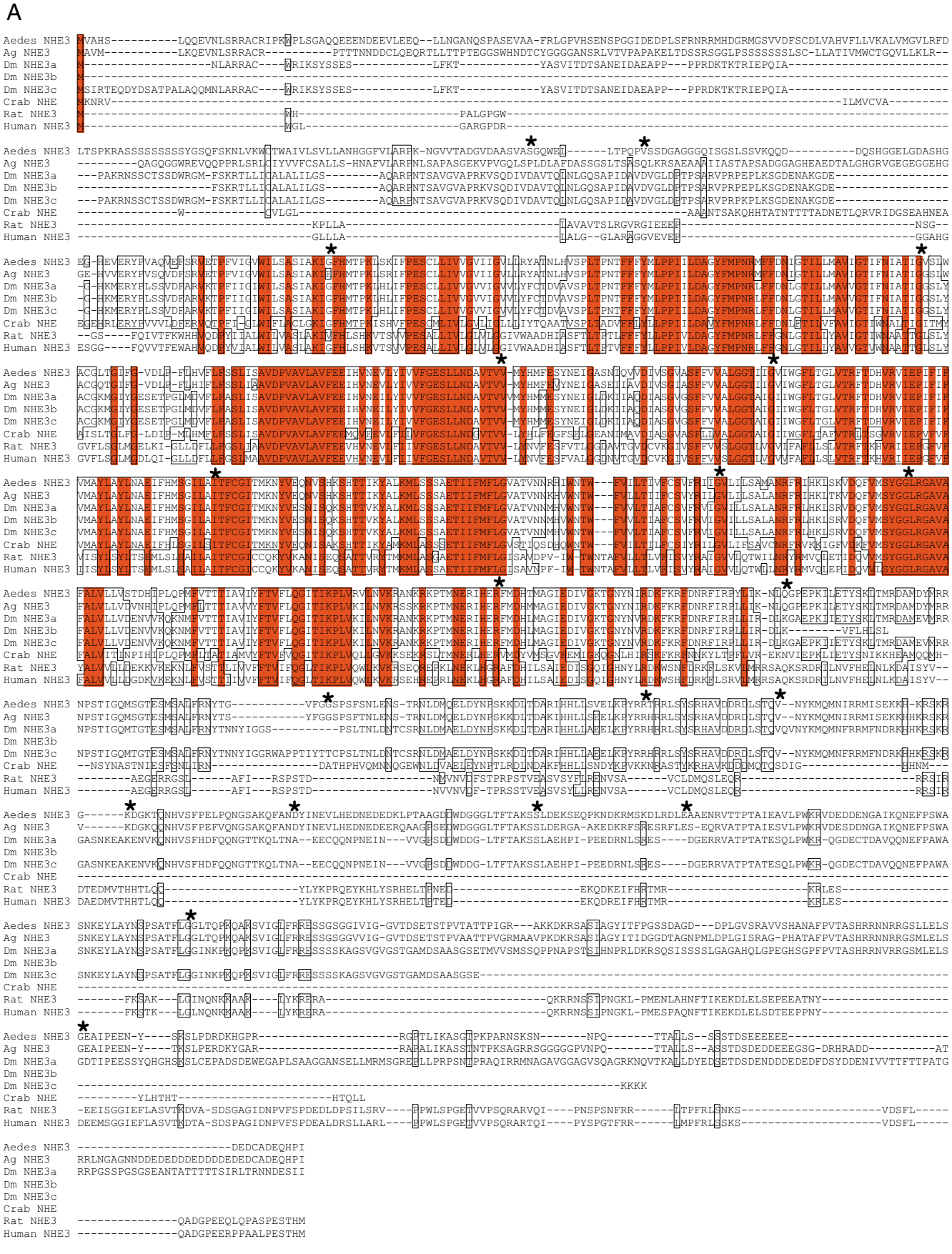
Aedes NHE3
Ag NHE3
Dm NHE3a
Dm NHE3b
Dm NHE3c
Crab NHE
Rat NHE3
Human NHE3

Fig. 1A.

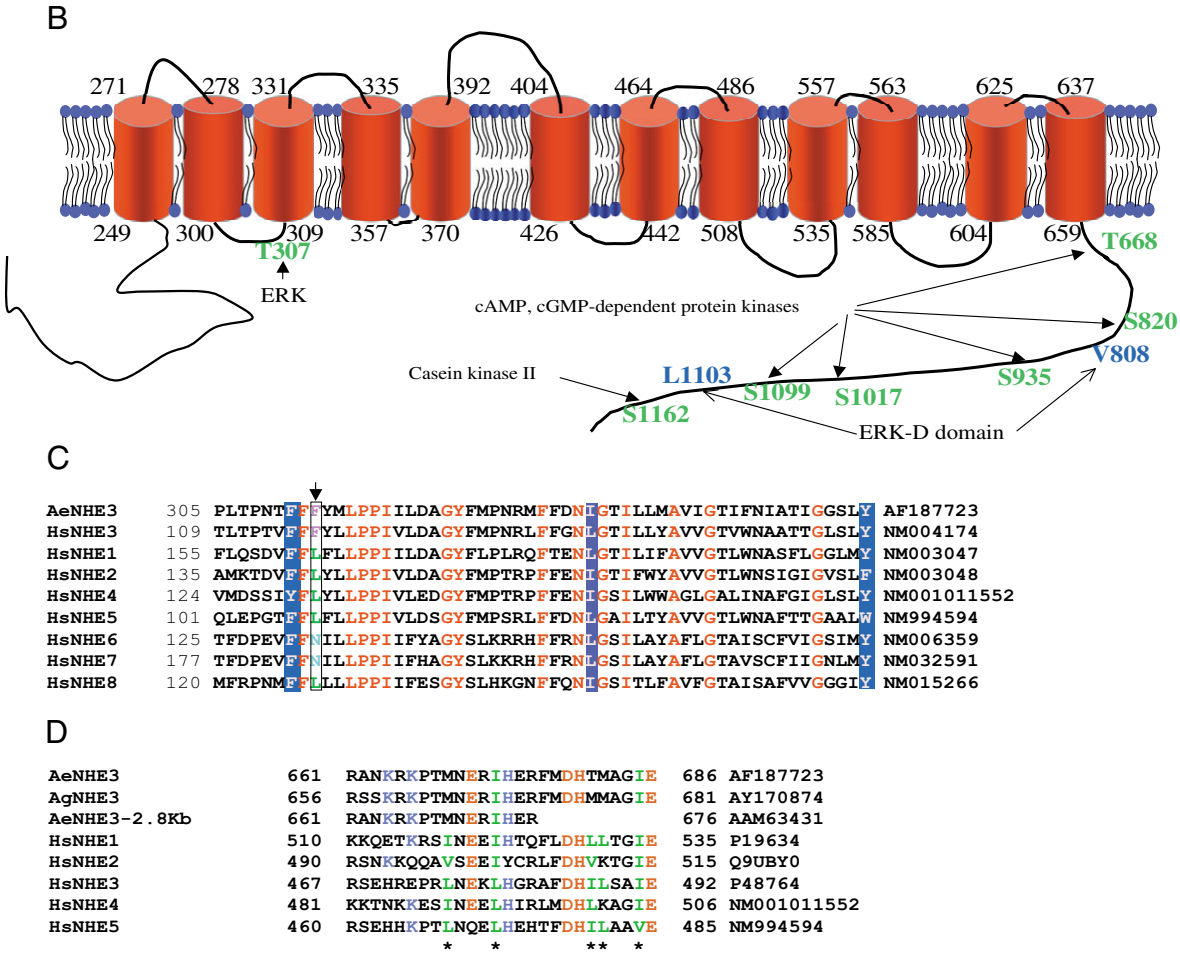

Fig. 1. Sequence and topology of the sodium/proton exchanger, NHE3 from *Aedes aegypti*. (A) Canonical translation of *Aedes* NHE3 (AF187723) aligned with *Anopheles* NHE3 (AY170874) and their close relatives in *Drosophila*, crab and vertebrates. DmNHE3a (AAF60313) refers to the full-length *Drosophila* NHE3 homolog, whereas DmNHE3b (AY048581) and DmNHE3c (AY128467) refer to possible splice variants identified by high-throughput cDNA sequencing and by RT-PCR analysis, respectively. Identical residues are shaded in red and conserved residues are boxed. DmNHE2 from the original annotation (Giannakou and Dow, 2001) is here assigned to the NHE3 family. *Ae*NHE3 ORF is encoded by 21 exons; asterisks indicate the position of introns. (B) Predicted transmembrane topology and potential phosphorylation sites in *Ae*NHE3. The positions of residues at the beginning and end of predicted transmembrane helices are numbered. Putative phosphorylation sites and ERK-D domains are given in green and blue, respectively. (C) Comparison of amiloride binding sites in NHEs. A critical leucine (arrow) within the pocket renders amiloride sensitivity to vertebrate NHE1, 2 and 4. The corresponding residue in *Ae*NHE3 is phenylalanine (F313). Substitution of leucine to phenylalanine in vertebrate NHE1 and 2 removes the amiloride sensitivity in these NHEs (see Discussion). Conserved residues are shown in red whereas semi-conservative substitutions are back-shadowed in blue. (D) Calcineurin B homologous protein (CHP) binding site is conserved in insect NHE3. The conserved hydrophobic residues (green) are required for efficient transport function of plasma membrane NHEs. Note that the shorter *Ae*NHE3 (AeNHE3-2.8kb) contains only half-site for CHP binding. Ae, Ag and Hs refer to *Aedes aegypti*, *Anopheles gambiae* and human, respectively. Accession numbers (GenBank; right) and amino acid positions (left) are indicated.

was much higher in the rectum where reabsorption of fluid and ions are known to occur in a variety of insects (Fig. 4G).

Functional characterization of Aedes NHE3

Yeast AXT3 cells that lack the Na^+ efflux proteins ENA1–4, the plasma membrane Na^+/H^+ antiporter NHA1 and the vacuolar antiporter NHX1 are very sensitive to high sodium in growth media (Madrid et al., 1998; Quintero et al., 2000). Their salt-sensitive phenotype makes them a convenient tool for studying Na^+ extrusion and/or sequestration ability of NHE-like proteins by heterologous protein expression. When *Ae*NHE3 was expressed in this yeast strain under the control of the strong GAL 1 promoter, it restored salt tolerance at up to 70 mmol l^{-1} sodium (Fig. 5A and data not shown), but failed to restore tolerance to hygromycin B (Fig. 5B). Thus, *Ae*NHE3 rescues yeast plasma membrane NHE defects but does not complement vacuolar NHE (NHX) (see Discussion).

To further characterize *Ae*NHE3 function, PS120 cells selected by H^+-suicide that have been shown to lack a functional NHE (Pouyssegur et al., 1984) were used. These cells are conditional for growth in HCO_3^--free medium and

lose viability in neutral and acidic pH (Pouyssegur et al., 1984). We selected *Ae*NHE3-expressing cells by transfection and double selection in conditional medium. To avoid selecting spontaneous revertants, selected clones were screened for GFP fluorescence encoded by a non-contiguous gene under independent promoter control in the cloning vector, pXOON. All selected clones were positive for GFP and no clones survived acid load when transfected with the empty vector alone. We did not detect any spontaneous revertants in untransfected cells or in those transfected with pXOON alone.

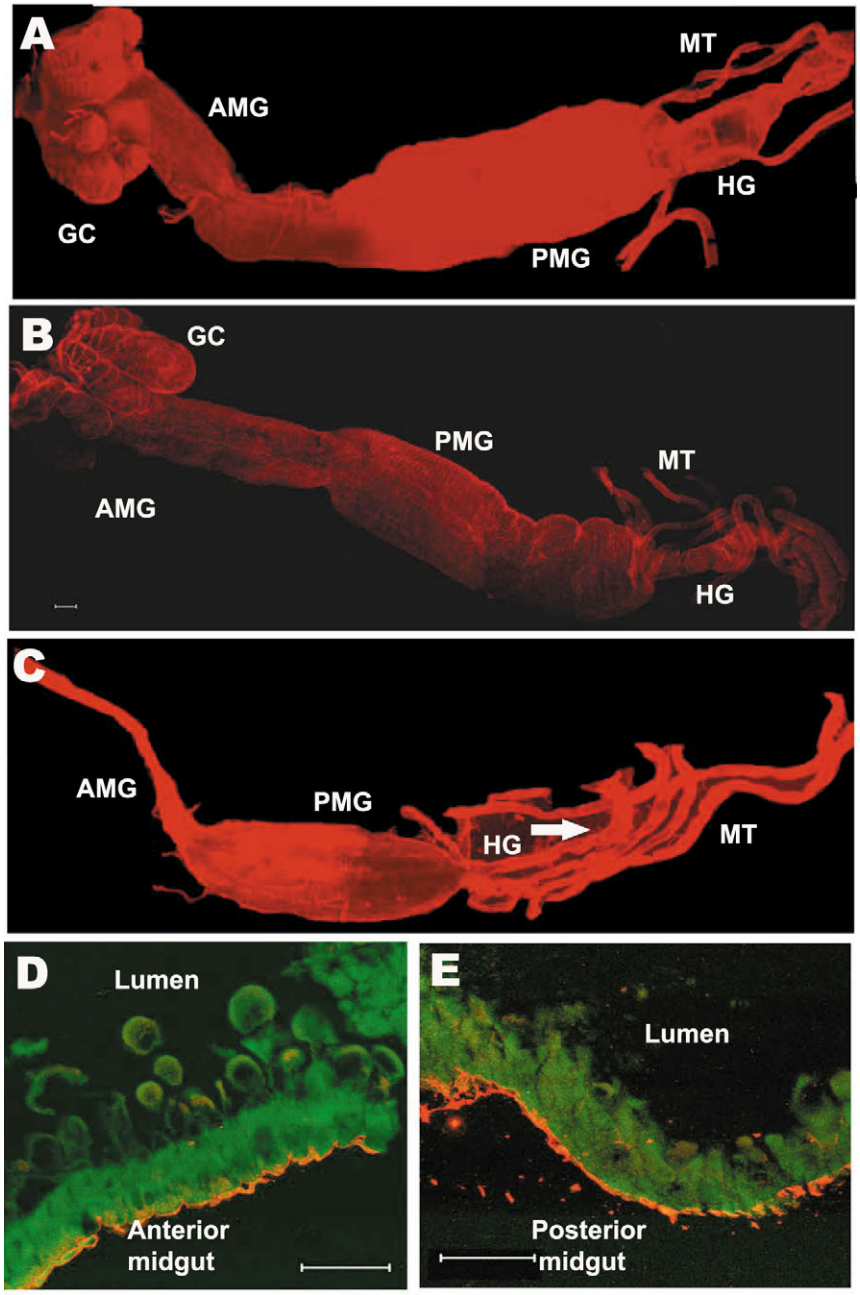

Fig. 2. Expression and localization of *Ae*NHE3 in osmoregulatory organs in larva and adult *Aedes aegypti*. *Ae*NHE3 is highly expressed in the posterior midgut (PMG) of larval (A) and adult (C) *Aedes aegypti*. Malpighian tubules (MT) and hindgut (HG) also show high *Ae*NHE3 immunoreactivity (red). In larva, anterior midgut (AMG) expresses lower levels of NHE3 whereas adult AMG expresses levels comparable to PMG. Interestingly, the distal part of adult PMG shows reduced expression of NHE3. In both anterior (D) and posterior (E) midgut, NHE3 expression (red) is restricted to the basolateral membrane. Actin in D and E is stained green. (B) The background fluorescence with preimmune serum used as primary antibody. Immune antibody preabsorbed with the peptide used for immunization gave similar results as in B. Scale bars, 100 μm (B); 50 μm (D,E).

Following an acid load, untransfected cells do not recover intracellular pH whereas unchallenged cells maintained in culture medium retain a near neutral pH (Fig. 6A). Polyclonal cells expressing *Ae*NHE3 were capable of alkalinization following an acid load and subsequent change to Na^+-buffer (Fig. 6B). We selected stable clones expressing *Ae*NHE3 and assayed for intracellular pH recovery following an acid challenge (Fig. 6C). Our selection procedure included growth in bicarbonate-free medium buffered with 20 mmol l^{-1} Hepes, pH 6.9. This growth condition was lethal to untransfected PS120 cells that are incapable of elevating intracellular pH in the absence of the activity of NHE1 and its coupled Cl^-/HCO_3^- transporter. The fact that we were able to select clonal lines under this conditional regime indicated that *Ae*NHE3 was functional in PS120 cells, where it functions in a manner similar to vertebrate NHE1 (Pouyssegur et al., 1984). Consistent with growth under non-permissive conditions in yeast AXT3 cells, *Ae*NHE3-expressing PS120 cells recovered intracellular pH after an acid load (compare Fig. 6A, grey bar, with Fig. 6C).

In order to determine if the large cytoplasmic carboxy tail is required for *Ae*NHE3 function we deleted the carboxy cytoplasmic tail of *Ae*NHE (NHE-CΔ) and assayed for its capacity to recover intracellular pH following an acid load (Fig. 6D). In all cases, recovery was not significantly compromised, indicating that the cytoplasmic tail is not essential for NHE3 function, but could be required for functions that are distinct from ion and proton translocation or required for regulating its activity in response to cellular cues in mosquito tissues that are not recapitulated in this mammalian expression system.

$^{22}Na^+$ uptake in AeNHE3 expressing cells is insensitive to amiloride and its derivative EIPA

Transiently transfected PS120 cells were

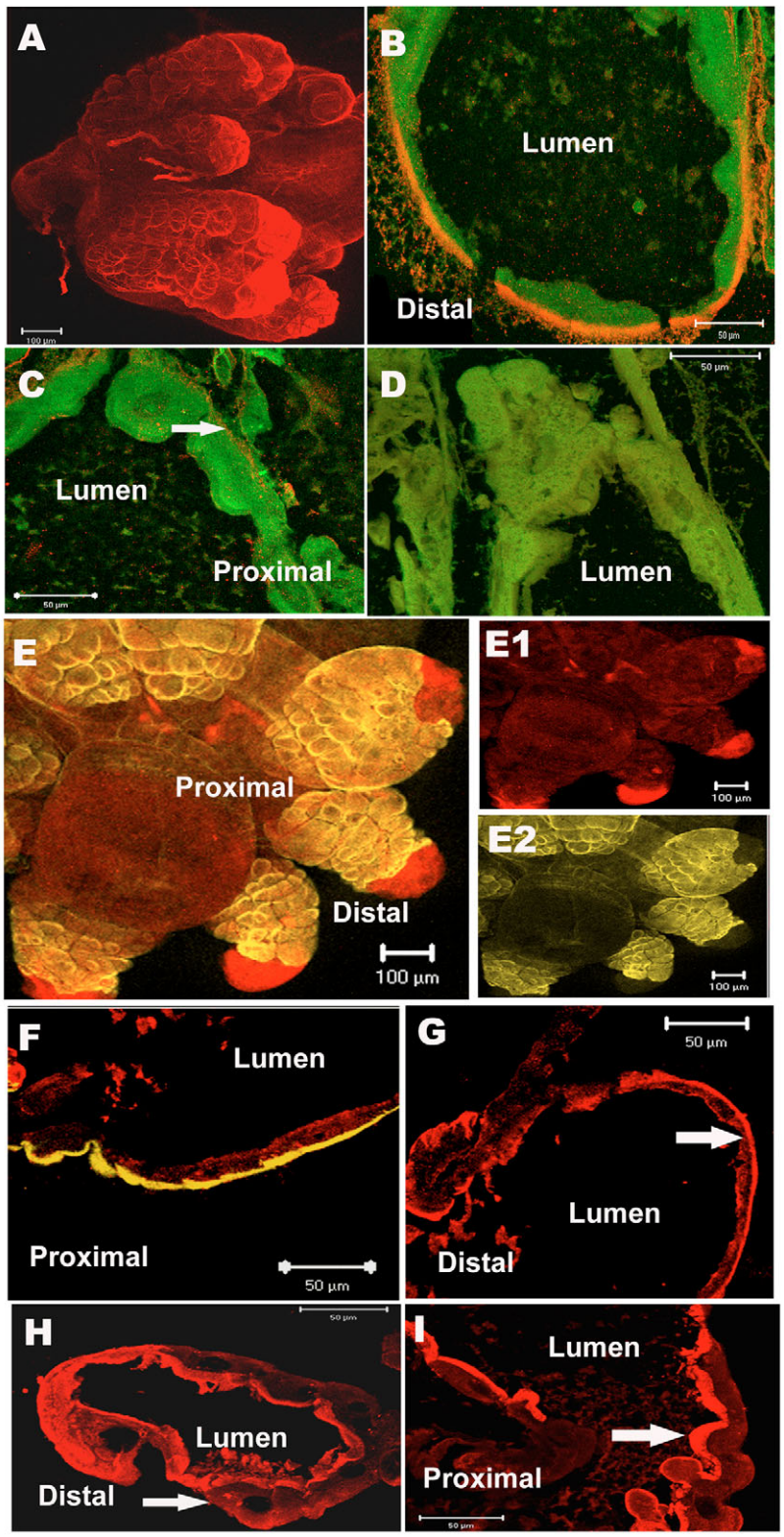

Fig. 3. Expression of NHE3, Na^+/K^+-ATPase and V-ATPase in the gastric caeca of larval *Aedes aegypti*. *Ae*NHE3 is highly expressed in the distal segment of gastric caeca (A) predominantly in the basolateral membrane (orange in B) of distal segment. Only faint labeling of NHE3 was found in the proximal segment of caeca (C, arrow). Na^+/K^+-ATPase is excluded from regions of higher NHE3 expression but is enriched in proximal segment (yellow in E) and is localized to the basolateral membrane (yellow in F). V-ATPase localizes to the apical plasma membrane of both proximal and distal parts of the gastric caeca (H,I). Weaker V-ATPase labeling was found in the distal basal membrane (arrow in H). Gastric caeca was labeled with anti-NHE3 antibody alone (A–C) (red in A, orange in B,C) or together (red in E-G) with anti-Na^+/K^+-ATPase monoclonal antibody (yellow in E–G). To visualize structures, actin was labeled with Alexa Fluor 488-phalloidin in B–D (green). Expression of the V-ATPase was detected with polyclonal antibodies to the B-subunit (H,I). Preimmune serum was used as negative control (D) with phalloidin (green). Immunohistochemistry was performed on whole mounts (A,E) or tissue sections as described in Materials and methods. E1 (red for NHE3) and E2 (yellow for Na^+/K^+-ATPase) show the separate channels that are merged in E. F and G are similarly merged images of dual labeling with NHE 3 (red) and Na^+/K^+-ATPase (yellow) antibodies. Scale bars, 100 µm (E,E1,E2); 50 µm (A–D,F–I).

assayed for $^{22}Na^+$ uptake in 12- or 24-well formats. Cells were either transfected with the vector alone (control) or with those expressing the full-length *Ae*NHE3 ORF and assayed for sodium uptake following an acid load protocol. To determine the sensitivity of $^{22}Na^+$ uptake by *Ae*NHE3 to amiloride and its analog we compared these agents at concentrations that were sufficient to completely inhibit mammalian NHE1. In the presence of 1 mmol l^{-1} amiloride or 100 µmol l^{-1} EIPA, concentrations that completely abolish mammalian NHE1 mediated functions (Orlowski, 1993), $^{22}Na^+$ uptake was only reduced by 40%, showing that *Ae*NHE3 is at best partially sensitive to amiloride and EIPA at very high concentrations (Fig. 7A). No further change in sensitivity to amiloride or EIPA was evident in cells lacking the carboxy tail of NHE3 (NHE-CΔ) (Fig. 7B). We conclude that the large cytoplasmic region of NHE3 is dispensable for its sodium transport function, similar to its proton translocation properties. However, this does not preclude the possibility that this region might possess subtle functional attributes by sensitizing the exchanger to small and transient changes in pH or other cellular aspects that are not reproduced in this vertebrate cell line. The data are consistent with the model that *Ae*NHE3 is insensitive to traditional agents used to distinguish the contribution of several NHEs in Na^+ and proton transport across membranes. Further, the transport properties require only the core domain of NHEs consisting of the transmembrane helices.

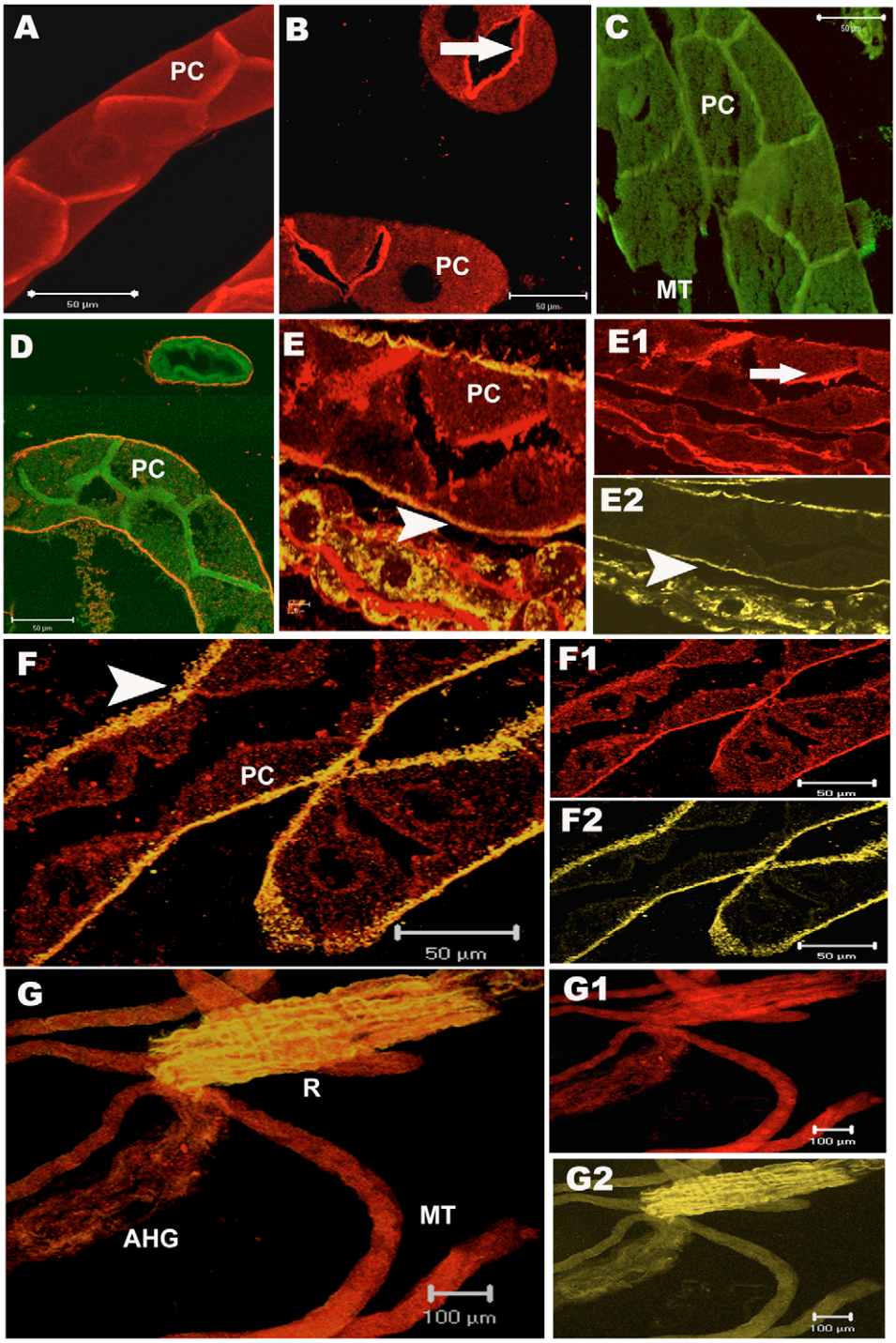

Fig. 4. Expression of *Ae*NHE3, Na^+/K^+-ATPase and V-ATPase in the Malpighian tubules and hindgut of *Aedes aegypti*. Whole-mount (A,G) or paraffin sections (B–F) were analyzed by labeling with V-ATPase B-subunit (A,B), anti-NHE3 antibody (D–G) and anti-Na^+/K^+-ATPase α1 subunit monoclonal antibody (E–G). Preimmune serum was used as negative control (C) with phalloidin (green), and similar results were obtained with peptide preabsorbed anti-NHE3 antibody. V-ATPase is primarily localized to the apical membrane of principal cells (PC in A,B) whereas both NHE3 (D,F) and Na^+/K^+-ATPase (F) localize to basal aspect of the plasma membrane of principal cells. In median Malpighian tubules NHE3 expression was also detected in the apical membrane (E, arrow) and in the basal membrane colocalizing with Na^+/K^+-ATPase (E, arrowhead). Weaker expression of NHE3 was also detected as punctate structures in the cytoplasm of Malpighian tubules (F,F1). Anterior hindgut and Malpighian tubules exhibit similar expression levels of NHE3, whereas in the rectum both NHE3 and Na^+/K^+-ATPase are remarkably enhanced (G,G1,G2). E1,F1,G1 show NHE3 expression (red), while E2,F2,G2 depict Na^+/K^+-ATPase expression (yellow), and merged channels depicting co-localization of NHE3 and Na^+/K^+-ATPase are shown in E–G. Scale bars, 50 µm (A–F); 100 µm (G).

Discussion

Here we report the cloning, tissue distribution, subcellular localization and functional characterization of an *Aedes aegypti* NHE3. High millimolar concentrations of sodium are toxic to the yeast, *S. cerevisiae*, and must be extruded through the plasma membrane (Rodriguez-Navarro et al., 1994), or sequestered in vacuoles (Darley et al., 2000). The four plasma membrane Na^+-ATPases (ENA1–4) (Darley et al., 2000) and the plasma membrane Na^+/H^+ antiporter NHA1 (Prior et al., 1996) extrude sodium from the cells; the vacuolar exchanger NHX1 (Nass et al., 1997), on the other hand, sequesters it in vacuoles. AXT3 yeast cells have disruptions on ENA1–4, NHA1 and NHX1 genes, which render the strain highly sensitive to high sodium levels (Quintero et al., 2000). In addition, the functionality of vacuolar NHX1 can be determined by assaying the yeast cells' tolerance to hygromycin B; the precise mechanism by which NHX1 imparts this resistance is, however, not yet well understood (Gaxiola et

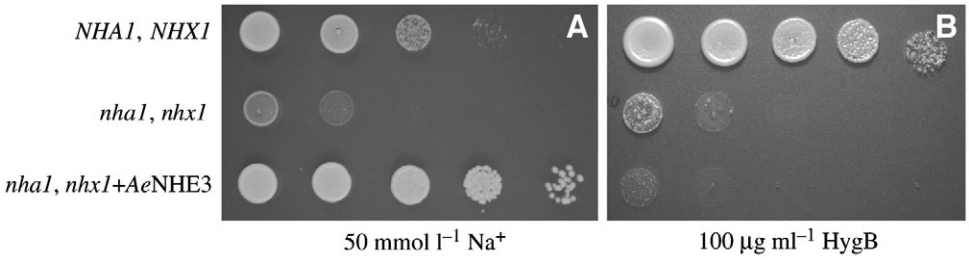

Fig. 5. *Ae*NHE3 rescues *S. cerevisiae NHA1* function when heterologously expressed in mutant cells lacking endogenous Na^+ efflux and Na^+/H^+ exchanger proteins. Yeast cells were grown in alkali cation free-AP medium overnight, and cell density adjusted to an OD_{600}=1. Tenfold serial decimal dilutions were spotted on: (A) AP plates containing 50 mmol l^{-1} NaCl, and (B) minimal media plates containing 100 μg ml^{-1} Hygromycin B. Growth was recorded after 4 days in (A), and 3 days in (B). Strain G19 was used as the *NHA1*, *NHX1* wild-type control; *nha1*, *nhx1* is the AXT3 strain. *Ae*NHE3 expression was under galactose induction; all controls were transformed with an empty vector.

al., 1999). *Ae*NHE3 on expression in AXT3 cells conferred sodium-tolerance to a concentration as high as 70 mmol l^{-1} (Fig. 5 and data not shown), but offered no improvement in growth in media containing 100 μg ml^{-1} hygromycin B. This indicates that the mosquito exchanger is not functional in vacuoles, and any salt-tolerance conferred on the mutant cells would be attributable to plasma membrane Na^+/H^+ exchange. Wild-type yeast cells can grow in media with a sodium concentration as high as 200 mmol l^{-1} (Quintero et al., 2000). This genetic complementation assay adds to previous findings on *Ae. aegypti* NHE8 (W.K., A.K.P., K.A. and S.S.G., manuscript submitted for publication) showing that the genetic pliability of yeast eases the functional characterization of proteins, from organisms that are more difficult to manipulate such as the mosquitoes.

In insects, the Malpighian tubules, gastric caeca, midgut and hindgut are organs involved in fluid and ion homeostasis. Immunolocalization studies with an antibody to the carboxy tail epitope of NHE3 indicate that *Ae*NHE3 is localized in almost all tissues examined, predominantly to the basal membrane. Interestingly, we also detected apically localized NHE3 in the median segment of Malpighian tubule (Fig. 4). Further, intracellular staining in Malpighian tubules is suggestive of NHE3 being sequestered in endomembrane compartments, likely representing the population being recycled through endocytosis. The different localization patterns of NHE3 might reflect its functional versatility. The basolateral localization of NHE3 was surprising since vertebrate NHE3 is expressed in apical membranes of renal tissues, apart from a distinct cytoplasmic pool (Biemesderfer et al., 1997; Chow et al., 1999; D'Souza et al., 1998; Janecki et al., 1998) that is recruited to the apical membrane in a phosphatidylinositol 3-kinase dependent manner (Kurashima et al., 1998). Thus, *Ae*NHE3 seems to share a localization pattern similar to the vertebrate 'housekeeping' NHE1 that resides in the basolateral membrane and also to vertebrate NHE3 that is present both in apical membrane and in endomembrane compartments. Future work should clarify the complex trafficking patterns that underlie NHE3 localization, dynamics and function in tubule physiology.

In his classical work in *Aedes* larvae, Ramsay showed that the midgut region corresponding to the 3–5 abdominal segment to be involved in ion and fluid transport (Ramsay, 1951). Our results demonstrating the presence and enrichment of NHE3 precisely to that location in the midgut (Fig. 2) (Clements, 1992) support the possibility that NHE3 activity may play a role in ionic homeostasis in the midgut. This possibility is further strengthened by the expression pattern of NHE3 in gastric caeca (Fig. 3). Two distinct segments of the gastric caeca are known for ion and fluid transport. Reabsorbing/secreting cells (at proximal caeca) and ion transporting cells (at distal caeca) have been identified where secondary concentration and fluid secretion occur (Clements, 1992; Ramsay, 1950; Ramsay, 1951; Volkmann and Peters, 1989a; Volkmann and Peters, 1989b). Higher levels of NHE3 expression in distal gastric caeca thus might be reflective of NHE3's role in ion and proton exchange in the caeca. The proximal segment of gastric caeca expressed lower levels of NHE3, in contrast to Na^+/K^+-ATPase. Together with expression of V-ATPase in distal gastric caeca, our present results support the model for ion transport in insect epithelium where a V-ATPase and its coupled cation/H^+ transporter constitute the major fluid and ion transport mechanism. However, both components of this pump are proposed to be located in the apical membrane, with little consideration given to a basolateral Na^+/H^+ exchanger. Because NHE3 is expressed in the basolateral membrane of gastric caeca and most of Malpighian tubules, we believe this isoform does not constitute the tightly coupled exchanger operating in parallel with V-ATPase in gastric caeca and most of the tubules. However, it is possible that homologue(s) of one of the other four NHEs identified by *in silico* methods (Pullikuth et al., 2003) or the recently characterized exchanger (W.K., A.K.P., K.A. and S.S.G., manuscript submitted for publication) might constitute the exchanger coupled to the apical membrane proton pump. In addition, we cannot rule out an equally likely possibility that *Ae*NHE3 might, by virtue of its basolateral localization, play a role in regulating intracellular pH that indirectly impacts V-ATPase and apical exchanger functions.

Drosophila NHE3 contains three splice variants, DmNHE3a, b and c. A shorter variant of NHE3 (here named *Ae*NHE3b) was recently identified that is possibly expressed in Malpighian tubules (Hart et al., 2002). This splice variant results in a protein of 672 amino acids that lacks most of the carboxy cytoplasmic tail. The C-terminal deletion mutant of *Ae*NHE3 (NHE3ΔC) is analogous to the shorter version identified

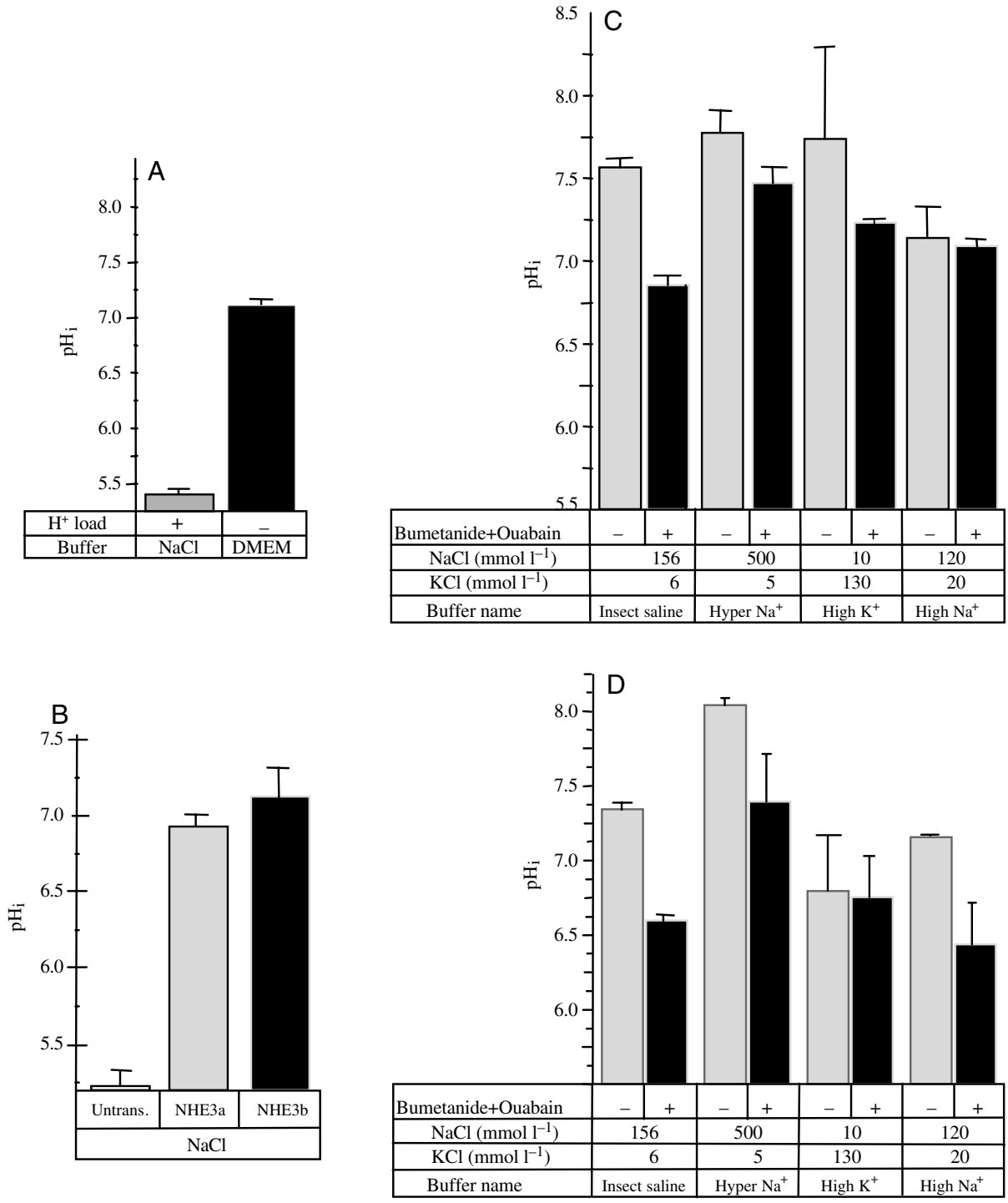

Fig. 6. Functional characterization of *Ae*NHE3 in a NHE-deficient cell line. (A) Untransfected PS120 cells fail to recover intracellular pH following an acid load, but maintain a near neutral pH in culture medium (DMEM). Cells were challenged with a H^+ load (+) or left unchallenged (–) and subsequently changed to buffer (135 mmol l^{-1} NaCl, HBS, pH 7.4) or culture medium (DMEM) and assayed by ratiometric fluorimetry. (B) Polyclonal cells from two separate transfection experiments (NHE3a and NHE3b) expressing full-length *Ae*NHE3 were subjected to acid load and recovery of intracellular pH was monitored by BCECF fluorescence. (C) A stable clone (clone A2) expressing *Ae*NHE3 was subjected to acid load and changed to buffers containing the indicated concentrations of ions to monitor change in intracellular pH (pH_i) with (+) or without (–) inhibitors of Na^+/K^+-ATPase (1 mmol l^{-1} ouabain) and $Na^+/K^+/Cl^-$ cotransporter (100 μmol l^{-1} bumetanide). Experiments with another stable clone (clone B3) produced similar results. (D) The cytoplasmic carboxy terminal of *Ae*NHE3 is not required for its function. A stable clone (NHE CΔ-clone A8) that expresses *Ae*NHE CΔ (lacking carboxy 448 amino acids) was assayed for pH_i recovery after an acid load in the presence or absence of inhibitors as stated in C. Experiments with another stable line (NHE CΔ-clone B7) produced similar results. The buffers also contained 5 mmol l^{-1} glucose, 2 mmol l^{-1} $CaCl_2$ and 1 mmol l^{-1} $MgCl_2$. Values are means ± standard error (N=4–8).

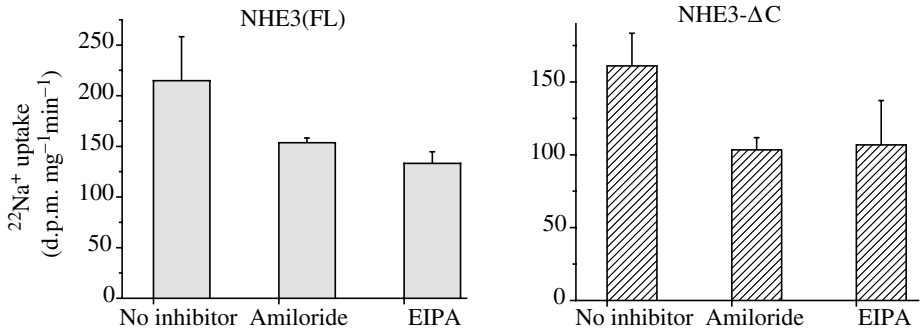

Fig. 7. Amiloride-insensitive $^{22}Na^+$-uptake in *Ae*NHE3-expressing fibroblast cell line. Full-length (NHE3FL) or carboxy-terminal truncated (NHE3ΔC) *Ae*NHE3 were transiently transfected into PS120 cells. 3–4 days after transfection, cells were assayed for $^{22}Na^+$ uptake in the presence of inhibitors (1 mmol l^{-1} amiloride or 100 μmol l^{-1} EIPA). Values are d.p.m. mg^{-1} protein min^{-1} (means ± s.e.m.).

previously (Hart et al., 2002) that contains a highly conserved protein kinase A phosphorylation site (S^{668} and S^{664} in *Aedes* and *Anopheles* NHE3, respectively), analogous to vertebrate S^{605} that is the prime target for cAMP-mediated acute inhibition of NHE3 function (Kurashima et al., 1997). In contrast, trout red blood cell βNHE is activated by cAMP, which stimulates PKA phosphorylation of S^{641} and S^{648} (Malapert et al., 1997). Although similar adjacent PKA sites (S^{659} and S^{664}) are present in *Anopheles* NHE3 (Pullikuth et al., 2003) (Fig. 1A), it remains to be determined if these sites are indeed phosphorylated in a cAMP-dependent manner and whether such phosphorylation regulates the activity of mosquito NHE3s. *Ae*NHE3 contains a CHP-binding motif in the cytoplasmic tail that is likely to regulate its transport function. The hydrophobic residues within this motif (asterisks in Fig. 1D) bind the ubiquitous CHP in vertebrate NHEs. Substitution of these hydrophobic residues with hydrophilic residues, while not affecting surface expression of NHE1-3, dramatically reduces transport of Na^+ through these exchangers (Pang et al., 2004). This raises an intriguing possibility that *Ae*NHE3 and the shorter *Ae*NHE3b (Hart et al., 2002) might be differentially regulated by CHP since the latter contains only a half-site for CHP binding.

Whole tubule electrophysiological and microfluorimetric studies have demonstrated that cAMP stimulates fluid secretion by *Ae. aegypti* Malpighian tubules (reviewed in Beyenbach, 1995; Pannabecker, 1995). This stimulation could occur by the cAMP mediated responses on the basolateral bumetanide-sensitive $Na^+/K^+/Cl^-$ cotransporter, or by increasing basolateral Na^+ conductance (Beyenbach, 1995; Petzel, 2000; Petzel et al., 1999; Sawyer and Beyenbach, 1985; Williams and Beyenbach, 1984). The NHE antagonist amiloride inhibits basal secretion by isolated Malpighian tubules of *Ae. aegypti* (Hegarty et al., 1991) as well as serotonin-stimulated secretion by *Rhodnius prolixus* tubules (Maddrell and O'Donnell, 1992). However, amiloride had little effect on basal membrane voltages or transepithelial resistance, suggesting this Na^+ conductive pathway is amiloride-resistant (Hegarty et al., 1991). Basolateral Na^+ conductance is unlikely to occur through Na^+ channels since a recent RT-PCR analysis indicated that no Na^+ channels are expressed in Malpighian tubules of *Drosophila* (Giannakou and Dow, 2001). The effect of amiloride thus could be on the apical membrane NHE, which acts as secondary cation transport coupled to the bafilomycin-sensitive active transport of H^+ into the lumen by V-ATPase (Beyenbach et al., 2000; Pannabecker, 1995).

Current models propose an active apical proton pump coupled to a cation/H^+ exchanger as the primary generator of transepithelial gradients that facilitate fluid secretion in insect epithelia (Wieczorek et al., 1991). A basolateral NHE has not been implicated in contributing to this fluid secretion. However, our immunolocalization data clearly show that NHE3 is indeed localized to the basal membrane, where it can mediate Na^+ conductance that so far has been attributed to unidentified amiloride-resistant Na^+ channels (Hegarty et al., 1991). As amiloride has been the only means of distinguishing the activity and requirement of NHEs in these studies, specific NHEs resistant or insensitive to these antagonists would mask their cellular relevance in fluid and ion secretion and in maintenance of intracellular pH. We showed the $^{22}Na^+$ uptake of *Ae*NHE3 to be insensitive to amiloride and its anologue, EIPA (Fig. 7). These agents reduced uptake through *Ae*NHE3 by only 40%, whereas at similar concentrations completely abolish uptake and pH recovery by amiloride-sensitive mammalian NHEs (Orlowski, 1993). Further, Malpighian tubules of *Drosophila* and *Ae. aegypti* exhibited profound sensitivities to these agents under an acid load protocol (Giannakou and Dow, 2001; Petzel, 2000). We conclude that the sensitivity to inhibitors in these tissues does not reflect the transport function mediated by NHE3, which could transport Na^+ at the basolateral membrane and whose contribution cannot be unmasked with inhibitors that alter the properties of apical NHEs that are as yet undiscovered.

Accordingly, the very highly conserved leucine residue in the amiloride-binding pocket (FF**L**YLLPP) is substituted by phenyalanine (F313) in *Ae*NHE3 (arrow in Fig. 1C). A single site mutation (L167F) in the amiloride-sensitive vertebrate NHE1 renders it 30-fold resistant to the amiloride analog, methylpropyl amiloride (Counillon et al., 1993). Similarly, a mutant form of mammalian NHE2 (L143F) is 5- and 20-fold resistant to amiloride and EIPA, respectively, compared to wild-type NHE2 (Yun et al., 1993). In *Ae*NHE3, this residue corresponds to F313 (Fig. 1A,C), which is also conserved in the amiloride-resistant vertebrate NHE3 (F116). Our direct evidence for amiloride insensitivity of *Ae*NHE3 expressed in PS120 cells indicates that NHE3 function in basal membranes of Malpighian tubules is likely to be amiloride resistant. As a result, prevailing models of ion transport in Malpighian tubules

discounted the relevance of a basolateral NHE. We suggest fluid secretion in the Malpighian tubule of *Ae. aegypti* might involve ion and proton fluxes through the amiloride-resistant NHE3 located at the basolateral membrane.

The insect epithelial ion transport models suggest a K^+/H^+ or Na^+/H^+ exchanger situated in the apical membrane functions in reverse compared to physiological polarity of vertebrate NHEs (Beyenbach, 1995; Maddrell and O'Donnell, 1992; Pannabecker, 1995; Wessing et al., 1993; Wieczorek, 1992; Wieczorek et al., 2000). Protons extruded into the lumen by V-ATPase are taken into the cell in exchange for cellular Na^+ or K^+. Together with our results demonstrating NHE3 in the basolateral membranes, it is apparent that basal and apical NHEs need to operate in reverse orientation to each other to effect transepithelial ion transport. We demonstrated this directly by expressing *Ae*NHE3 in NHE1-deficient epithelial cell line (Figs 6 and 7). After an acid load, the cell interior was estimated to be less than pH 5.5. Upon exchange with Na^+- or K^+-rich solutions, *Ae*NHE3 expression resulted in efficient cellular alkalinization that showed no remarkable preference for Na^+ over K^+ or *vice versa*. Thus, *Ae*NHE3 is capable of assuming a transport polarity similar to vertebrate NHEs in aiding the extrusion of cellular protons in exchange for extracellular cation(s). It is reasonable to suggest that *Ae*NHE3 could function in a similar manner in the basolateral membrane of Malpighian tubule, gastric caeca and midgut of this mosquito.

Current models for ion and fluid secretion by Malpighian tubules are derived from studies on whole tubule physiology where regional specialization and functional correlation are not sufficiently delineated. We showed that distinct segments along the length of the tubule differ in their pattern of NHE3 expression and localization, which is likely to be the case for other transport proteins as well. These results suggest the need to re-evaluate unified models attempting to explain ion regulation in different parts of the Malpighian tubules. We hypothesize that fluid, proton and ion secretions by Malpighian tubules may require NHE3 activity in the basolateral membrane in the proximal and distal segments, whereas in the median segment of the tubule NHE3 can function additionally in the apical membrane where it might be regulated through recycling pathways.

In summary, we have characterized the *Ae*NHE3 that is localized to the basolateral membrane of almost all tissues examined in *Ae. aegypti*. The presence of potential splice variants, apical staining in median Malpighian tubule, and intracellular pool of NHE3 immunoreactivity, support the possibility that distinct isoforms could act in concert with differential transport polarity in insect epithelia. Our results add an important, yet often neglected, aspect of basolateral NHE function in models describing insect epithelial ion transport. Further efforts in distinguishing pharmacological properties, and molecular identification of the remaining NHE isoforms and their specific localization and expression dynamics should clarify the roles of these integral membrane proteins in ionic homeostasis in insects.

List of abbreviations

AP	arginine phosphate
BSA	bovine serum albumin
CHP	calcineurin B homologous protein
DMSO	dimethyl sulfoxide
FBS	fetal bovine serum
HBS	Hepes-buffered saline
K-pump	potassium pump
Na^+/K^+-ATPase	sodium/potassium ATPase
NGS	normal goat serum
NHE	sodium–proton exchanger
NMDG	*N*-methyl-D-glucamine
ORF	open reading frame
PFA	paraformaldehyde
V-ATPase	vacuolar-type ATPase

We thank Dr Marjorie Patrick for suggesting the use of a5 Na^+/K^+-ATPase monoclonal antibody, Drs James Melvin, Jacques Pouysségur, Jose M. Pardo and Thomas Jespersen for sharing reagents with us. Research was funded through grants from the National Institutes of Health, AI 32572 and AI48049.

References

Adams, M. D., Celniker, S. E., Holt, R. A., Evans, C. A., Gocayne, J. D., Amanatides, P. G., Scherer, S. E., Li, P. W., Hoskins, R. A., Galle, R. F. et al. (2000). The genome sequence of *Drosophila melanogaster*. *Science* **287**, 2185-2195.

Attaphitaya, S., Park, K. and Melvin, J. E. (1999). Molecular cloning and functional expression of a rat Na^+/H^+ exchanger (NHE5) highly expressed in brain. *J. Biol. Chem.* **274**, 4383-4388.

Beyenbach, K. W. (1995). Mechanisms and regulation of electrolyte transport in Malpighian tubules. *J. Insect Physiol.* **41**, 197-207.

Beyenbach, K. W., Pannabecker, T. L. and Nagel, W. (2000). Central role of the apical membrane H^+-ATPase in electrogenesis and epithelial transport in Malpighian tubules. *J. Exp. Biol.* **203**, 1459-1468.

Biemesderfer, D., Pizzonia, J., Abu-Alfa, A., Exner, M., Reilly, R., Igarashi, P. and Aronson, P. S. (1993). NHE3: a Na^+/H^+ exchanger isoform of renal brush border. *Am. J. Physiol.* **265**, F736-F742.

Biemesderfer, D., Rutherford, P. A., Nagy, T., Pizzonia, J. H., Abu-Alfa, A. K. and Aronson, P. S. (1997). Monoclonal antibodies for high-resolution localization of NHE3 in adult and neonatal rat kidney. *Am. J. Physiol.* **273**, F289-F299.

Brant, S. R., Yun, C. H., Donowitz, M. and Tse, C. M. (1995). Cloning, tissue distribution, and functional analysis of the human Na^+/H^+ exchanger isoform, NHE3. *Am. J. Physiol.* **269**, C198-C206.

Burckhardt, G., Di Sole, F. and Helmle-Kolb, C. (2002). The Na^+/H^+ exchanger gene family. *J. Nephrol.* **15**, S3-S21.

Chow, C. W., Khurana, S., Woodside, M., Grinstein, S. and Orlowski, J. (1999). The epithelial Na(+)/H(+) exchanger, NHE3, is internalized through a clathrin-mediated pathway. *J. Biol. Chem.* **274**, 37551-37558.

Clements, A. N. (1992). *The Biology of Mosquitoes*. London: Chapman & Hall.

Counillon, L. and Pouyssegur, J. (2000). The expanding family of eucaryotic Na(+)/H(+) exchangers. *J. Biol. Chem.* **275**, 1-4.

Counillon, L., Franchi, A. and Pouyssegur, J. (1993). A point mutation of the Na^+/H^+ exchanger gene (NHE1) and amplification of the mutated allele confer amiloride resistance upon chronic acidosis. *Proc. Natl. Acad. Sci. USA* **90**, 4508-4512.

Darley, C. P., van Wuytswinkel, O. C., van der Woude, K., Mager, W. H. and de Boer, A. H. (2000). *Arabidopsis thaliana* and *Saccharomyces cerevisiae* NHX1 genes encode amiloride sensitive electroneutral Na^+/H^+ exchangers. *Biochem. J.* **351**, 241-249.

Dow, J. A. (1999). The multifunctional *Drosophila melanogaster* V-ATPase is encoded by a multigene family. *J. Bioenerg. Biomembr.* **31**, 75-83.

D'Souza, S., Garcia-Cabado, A., Yu, F., Teter, K., Lukacs, G., Skorecki,

K., Moore, H. P., Orlowski, J. and Grinstein, S. (1998). The epithelial sodium-hydrogen antiporter Na^+/H^+ exchanger 3 accumulates and is functional in recycling endosomes. *J. Biol. Chem.* **273**, 2035-2043.

Filippova, M., Ross, L. S. and Gill, S. S. (1998). Cloning of the V-ATPase B subunit cDNA from *Culex quinquefasciatus* and expression of the B and C subunits in mosquitoes. *Insect Mol. Biol.* **7**, 223-232.

Gaxiola, R. A., Rao, R., Sherman, A., Grisafi, P., Alper, S. L. and Fink, G. R. (1999). The *Arabidopsis thaliana* proton transporters, AtNhx1 and Avp1, can function in cation detoxification in yeast. *Proc. Natl. Acad. Sci. USA* **96**, 1480-1485.

Giannakou, M. E. and Dow, J. A. (2001). Characterization of the *Drosophila melanogaster* alkali-metal/proton exchanger (NHE) gene family. *J. Exp. Biol.* **204**, 3703-3716.

Grinstein, S. and Wieczorek, H. (1994). Cation antiports of animal plasma membranes. *J. Exp. Biol.* **196**, 307-318.

Hart, S. J., Knezetic, J. A. and Petzel, D. H. (2002). Cloning and tissue distribution of two Na^+/H^+ exchangers from the Malpighian tubules of *Aedes aegypti*. *Arch. Insect Biochem. Physiol.* **51**, 121-135.

Hegarty, J. L., Zhang, B., Pannabecker, T. L., Petzel, D. H., Baustian, M. D. and Beyenbach, K. W. (1991). Dibutyryl cAMP activates bumetanide-sensitive electrolyte transport in Malpighian tubules. *Am. J. Physiol.* **261**, C521-C529.

Hirokawa, T., Boon-Chieng, S. and Mitaku, S. (1998). SOSUI: classification and secondary structure prediction system for membrane proteins. *Bioinformatics* **14**, 378-379.

Holt, R. A., Subramanian, G. M., Halpern, A., Sutton, G. G., Charlab, R., Nusskern, D. R., Wincker, P., Clark, A. G., Ribeiro, J. M., Wides, R. et al. (2002). The genome sequence of the malaria mosquito *Anopheles gambiae*. *Science* **298**, 129-149.

Janecki, A. J., Montrose, M. H., Zimniak, P., Zweibaum, A., Tse, C. M., Khurana, S. and Donowitz, M. (1998). Subcellular redistribution is involved in acute regulation of the brush border Na^+/H^+ exchanger isoform 3 in human colon adenocarcinoma cell line Caco-2. Protein kinase C-mediated inhibition of the exchanger. *J. Biol. Chem.* **273**, 8790-8798.

Jespersen, T., Grunnet, M., Angelo, K., Klaerke, D. A. and Olesen, S. P. (2002). Dual-function vector for protein expression in both mammalian cells and *Xenopus laevis* oocytes. *Biotechniques* **32**, 536-540.

Kurashima, K., Yu, F. H., Cabado, A. G., Szabo, E. Z., Grinstein, S. and Orlowski, J. (1997). Identification of sites required for down-regulation of Na^+/H^+ exchanger NHE3 activity by cAMP-dependent protein kinase. phosphorylation-dependent and -independent mechanisms. *J. Biol. Chem.* **272**, 28672-28679.

Kurashima, K., Szabo, E. Z., Lukacs, G., Orlowski, J. and Grinstein, S. (1998). Endosomal recycling of the Na^+/H^+ exchanger NHE3 isoform is regulated by the phosphatidylinositol 3-kinase pathway. *J. Biol. Chem.* **273**, 20828-20836.

Maddrell, S. H. P. (1991). The fastest fluid-secreting cell known: the upper Malpighian tubule cell of *Rhodnius*. *BioEssays* **13**, 357-362.

Maddrell, S. H. and O'Donnell, M. J. (1992). Insect Malpighian tubules: V-ATPase action in ion and fluid transport. *J. Exp. Biol.* **172**, 417-429.

Madrid, R., Gomez, M. J., Ramos, J. and Rodriguez-Navarro, A. (1998). Ectopic potassium uptake in trk1 trk2 mutants of *Saccharomyces cerevisiae* correlates with a highly hyperpolarized membrane potential. *J. Biol. Chem.* **273**, 14838-14844.

Malapert, M., Guizouarn, H., Fievet, B., Jahns, R., Garcia-Romeu, F., Motais, R. and Borgese, F. (1997). Regulation of Na^+/H^+ antiporter in trout red blood cells. *J. Exp. Biol.* **200**, 353-360.

Nass, R., Cunningham, K. W. and Rao, R. (1997). Intracellular sequestration of sodium by a novel Na^+/H^+ exchanger in yeast is enhanced by mutations in the plasma membrane H^+-ATPase. Insights into mechanisms of sodium tolerance. *J. Biol. Chem.* **272**, 26145-26152.

Orlowski, J. (1993). Heterologous expression and functional properties of amiloride high affinity (NHE-1) and low affinity (NHE-3) isoforms of the rat Na/H exchanger. *J. Biol. Chem.* **268**, 16369-16377.

Orlowski, J. and Grinstein, S. (1997). Na^+/H^+ exchangers of mammalian cells. *J. Biol. Chem.* **272**, 22373-22376.

Orlowski, J. and Grinstein, S. (2004). Diversity of the mammalian sodium/proton exchanger SLC9 gene family. *Pflugers Arch.* **447**, 549-565.

Pang, T., Su, X., Wakabayashi, S. and Shigekawa, M. (2001). Calcineurin homologous protein as an essential cofactor for Na^+/H^+ exchangers. *J. Biol. Chem.* **276**, 17367-17372.

Pang, T., Hisamitsu, T., Mori, H., Shigekawa, M. and Wakabayashi, S. (2004). Role of calcineurin B homologous protein in pH regulation by the Na^+/H^+ exchanger 1, tightly bound Ca^+ ions as important structural elements. *Biochemistry* **43**, 3628-3636.

Pannabecker, T. (1995). Physiology of the Malpighian tubule. *Annu. Rev. Entomol.* **40**, 493-510.

Paris, S. and Pouyssegur, J. (1983). Biochemical characterization of the amiloride-sensitive Na^+/H^+ antiport in Chinese hamster lung fibroblasts. *J. Biol. Chem.* **258**, 3503-3508.

Petzel, D. H. (2000). Na(+)/H(+) exchange in mosquito Malpighian tubules. *Am. J. Physiol.* **279**, R1996-R2003.

Petzel, D. H., Hagedorn, H. H. and Beyenbach, K. W. (1986). Peptide nature of two mosquito natriuretic factors. *Am. J. Physiol.* **250**, R328-R332.

Petzel, D. H., Berg, M. M. and Beyenbach, K. W. (1987). Hormone-controlled cAMP-mediated fluid secretion in yellow-fever mosquito. *Am. J. Physiol.* **253**, R701-R711.

Petzel, D. H., Pirotte, P. T. and Van Kerkhove, E. (1999). Intracellular and luminal pH measurements of Malpighian tubules of the mosquito *Aedes aegypti*: the effects of cAMP. *J. Insect Physiol.* **45**, 973-982.

Pouyssegur, J., Sardet, C., Franchi, A., L'Allemain, G. and Paris, S. (1984). A specific mutation abolishing Na^+/H^+ antiport activity in hamster fibroblasts precludes growth at neutral and acidic pH. *Proc. Natl. Acad. Sci. USA* **81**, 4833-4837.

Prior, C., Potier, S., Souciet, J. L. and Sychrova, H. (1996). Characterization of the NHA1 gene encoding a Na^+/H^+-antiporter of the yeast *Saccharomyces cerevisiae. FEBS Lett.* **387**, 89-93.

Pullikuth, A. K., Filippov, V. and Gill, S. S. (2003). Phylogeny and cloning of ion transporters in mosquitoes. *J. Exp. Biol.* **206**, 3857-3868.

Quintero, F. J., Blatt, M. R. and Pardo, J. M. (2000). Functional conservation between yeast and plant endosomal Na(+)/H(+) antiporters. *FEBS Lett.* **471**, 224-228.

Ramsay, J. A. (1950). Osmotic regulation in mosquito larvae. *J. Exp. Biol.* **27**, 145-157.

Ramsay, J. A. (1951). Osmotic regulation in mosquito larvae: the role of the Malpighian tubules. *J. Exp. Biol.* **28**, 62-73.

Rodriguez-Navarro, A. and Ramos, J. (1984). Dual system for potassium transport in *Saccharomyces cerevisiae*. *J. Bacteriol.* **159**, 940-945.

Rodriguez-Navarro, A., Quintero, F. J. and Garciadeblas, B. (1994). Na(+)-ATPases and Na^+/H^+ antiporters in fungi. *Biochim. Biophys. Acta* **1187**, 203-205.

Ross, L. S. and Gill, S. S. (1996). Limited growth PCR screening of a plasmid library. *Biotechniques* **21**, 382-386.

Sawyer, D. B. and Beyenbach, K. (1985). Dibutyryl-cAMP increases basolateral sodium conductance of mosquito Malpighian tubules. *Am. J. Physiol.* **248**, R339-R345.

Takeyasu, K., Tamkun, M. M., Renaud, K. J. and Fambrough, D. M. (1988). Ouabain-sensitive (Na^+ + K^+)-ATPase activity expressed in mouse L cells by transfection with DNA encoding the alpha-subunit of an avian sodium pump. *J. Biol. Chem.* **263**, 4347-4354.

Tse, C. M., Levine, S. A., Yun, C. H., Brant, S. R., Pouyssegur, J., Montrose, M. H. and Donowitz, M. (1993). Functional characteristics of a cloned epithelial Na^+/H^+ exchanger (NHE3): resistance to amiloride and inhibition by protein kinase C. *Proc. Natl. Acad. Sci. USA* **90**, 9110-9114.

Volkmann, A. and Peters, W. (1989a). Investigations on the midgut caeca of mosquito larvae – I. Fine structure. *Tissue Cell* **21**, 243-251.

Volkmann, A. and Peters, W. (1989b). Investigations on the midgut caeca of mosquito larvae – II. Functional aspects. *Tissue Cell* **21**, 253-261.

Wakabayashi, S., Fafournoux, P., Sardet, C. and Pouyssegur, J. (1992). The Na^+/H^+ antiporter cytoplasmic domain mediates growth factor signals and controls 'H(+)-sensing'. *Proc. Natl. Acad. Sci. USA* **89**, 2424-2428.

Wessing, A., Bertram, G. and Zierold, K. (1993). Effects of bafilomucin A_1 and amiloride on the apical potassium and proton gradients in *Drosophila* Malpighian tubules studies by X-ray microanalysis and microelectrode measurements. *J. Comp. Physiol. B* **163**, 452-462.

Wieczorek, H. (1992). The insect V-ATPase, a plasma membrane proton pump energizing secondary active transport: molecular analysis of electrogenic potassium transport in the tobacco hornworm midgut. *J. Exp. Biol.* **172**, 335-343.

Wieczorek, H., Putzenlechner, M., Zeiske, W. and Klein, U. (1991). A vacuolar-type proton pump energizes K^+/H^+ antiport in an animal plasma membrane. *J. Biol. Chem.* **266**, 15340-15347.

Wieczorek, H., Brown, D., Grinstein, S., Ehrenfeld, J. and Harvey, W. R. (1999). Animal plasma membrane energization by proton-motive V-ATPases. *BioEssays* **21**, 637-648.

Wieczorek, H., Grber, G., Harvey, W. R., Huss, M., Merzendorfer, H. and Zeiske, W. (2000). Structure and regulation of insect plasma membrane H^+-V-ATPase. *J. Exp. Biol.* **203**, 127-135.

Wigglesworth, V. (1972). *Principles of Insect Physiology*. London: Chapman & Hall.

Williams, J. C. J. and Beyenbach, K. (1984). Differential effects of secretagogues on the electrophysiology of the Malpighian tubules of the yellow fever mosquito. *J. Comp. Physiol.* **154**, 301-309.

Yun, C. H., Little, P. J., Nath, S. K., Levine, S. A., Pouyssegur, J., Tse, C. M. and Donowitz, M. (1993). Leu143 in the putative fourth membrane spanning domain is critical for amiloride inhibition of an epithelial Na^+/H^+ exchanger isoform (NHE-2). *Biochem. Biophys. Res. Commun.* **193**, 532-539.

Zhang, G. H., Cragoe, E. J., Jr and Melvin, J. E. (1992). Regulation of cytoplasmic pH in rat sublingual mucous acini at rest and during muscarinic stimulation. *J. Membr. Biol.* **129**, 311-321.